Natural Magnetic Particles/Chitosan Impregnated with Silver Nanoparticles for Antibacterial Agents

Annisa Afra Martha, Defia Indah Permatasari, Elma Retna Dewi, Nikho Asyoka Wijaya, Eko Sri Kunarti, Bambang Rusdiarso, and Nuryono Nuryono*

Department of Chemistry, Faculty of Mathematics and Natural Sciences, Universitas Gadjah Mada, Sekip Utara, Yogyakarta 55281, Indonesia

Abstract: *In this research, silver nanoparticles (AgNP) impregnated on natural magnetic material/chitosan composite (NMP/Chi) have been conducted with different AgNP concentrations (0.5, 1.0, 1.5 mM). Their antibacterial activity was examined against* Escherichia coli *(E. coli) and* Staphylococcus aureus *(S. aureus). The AgNP samples were characterized with UV-Vis spectrophotometer and TEM. The NMP/Chi/AgNP samples were identified with FTIR and XRD, while NMP/Chi/AgNP1.0 (with the highest antibacterial activity) were analyzed with TEM and SEM-EDX. The antibacterial test with a well-diffusion method showed that NMP/Chi/AgNP was categorized as a strong antibacterial agent. The composite showing the largest inhibition zone diameters was NMP/Chi/AgNP prepared using 1.0 M AgNO₃, namely 14.39 and 16.8 mm against* E. coli *and* S. aureus, *respectively. Characterization of AgNP1.0 showed a spherical shape with an average particle diameter of 17.9 nm in suspension and 32.4 nm in NMP/Chi. The presence of 1000 mg/kg NMP/Chi/AgNP1.0 composite in water was able to reduce the growth of* E. coli *and* S. aureus *bacteria by 60.4% (from 5.3 to 2.1 CFU/mL) and 71.6% (from 6.34 to 1.86 CFU/mL), respectively, within 5 h. The NMP/Chi/AgNP1.0 showed an effective antibacterial agent against both bacteria (*E. coli *and* S. aureus*) and could be applied potentially in aquatic environments.*

***Keywords:** silver nanoparticle; antibacterial; composite; natural magnet; chitosan*

■ INTRODUCTION

Chlorination, ozonation, UV irradiation, photocatalytic degradation, and silver (Ag) metal have been widely used to deactivate wastewater's bacteria. Chlorination is a disinfection method using chlorine, acid, and hypochlorite ions. This process is effective but generates Cl_2 gas, which is mutagenic and carcinogenic to human health [1]. Ag metal has been known as an excellent antibacterial agent that inhibits growth and even kills bacteria, but its usage is required in large quantities and fancy. So, this can be overcome by producing Ag metal on a nanometer scale (ranging 1–10 nm) or embedded on the surface of the matrix materials [2]. In this way, only a small amount of Ag metal is used but more beneficial because Ag nanoparticles (AgNP) are more toxic for bacteria, especially *Escherichia coli* (*E. coli*)

and *Staphylococcus aureus* (*S. aureus*) [3]. In addition, there is no evidence that the microbes are resistant when exposed to silver nanoparticles.

The application of AgNP as antibacterial agents for aquatic environments possesses weakness. Namely, it cannot be re-usable since the agent is not easily separated from the media. Therefore, the impregnation of the AgNP on matrix materials is currently being developed. A natural matrix, like chitosan, revealed that antibacterial property is considerably capable of forming composites to produce a better antibacterial property. Chitosan, a polysaccharide obtained from the deacetylation of chitin, is used as an antibacterial agent due to its ability to interact with a negatively charged surface of a bacterial cell, disrupting the growth of bacterial growth colonies [4]. It can inhibit the pathogenic bacteria and spoilage

microorganisms, fungi, and gram-positive and -negative bacteria. Previous reports of the isolation and the excellent antibacterial property of chitosan from natural sources have been carried out [5]. In acidic conditions (pH < 6.5), a free amine group (–NH₂) of chitosan is protonated into a cationic amine group (–NH₃⁺) and can combine with various negatively charged materials, such as the surface of bacterial cells [6]. Chitosan attached to the magnetic materials causes to quickly separate it from the liquid medium after application using an external magnetic field. Chitosan coated on Fe_3O_4 surfaces aims to keep Fe_3O_4 stable, not readily oxidized, and not form aggregates. Chitosan is also known as toxic chelating metal. In addition, magnetite with nanometer size tends to aggregate to form bulk materials or form agglomerations caused by a decrease in surface energy. Aggregation can be prevented by coating the magnetite surface with a surfactant [7].

Besides synthetic, magnetic materials isolated from natural materials such as iron sand are currently applied [8], since material contains magnetic minerals such as magnetite (Fe_3O_4), hematite (α-Fe_2O_3), and maghemite (γ-Fe_2O_3) [9]. Iron sand is used as a source of Fe cation in the cobalt ferrite synthesis, which is less than 30 nm and is superparamagnetic. These sizes and properties make the resulting nanoparticles very good to be applied as an antibacterial agent. The magnetic property of iron sand can create a reused effect on the composite. Further, Fe_3O_4 magnetic material tends to be unstable and easily oxidized, so the composite formation is needed to overcome it. One of the composites used is chitosan. Chitosan is a natural polymer with charged sites due to electrolyte groups [10]. The synthesis of hybrid nanoparticles consisting of several components with a fine structure and excellent antibacterial properties has a high potential to be developed [11].

Magnetite nanoparticles mixed with polyaniline can be used as metal adsorbents, dyestuffs, or microwave absorbers [12]. Materials can be used as microwave absorbers due to their electrical and magnetic properties [13]. Several previous studies have shown that the antibacterial effectiveness of silver is higher when bound with Fe_3O_4. The Ag/Fe_3O_4 core-type nanoparticles showed antibacterial properties against bacterial strains such as *E.*

coli, *Staphylococcus epidermis*, and *Bacillus subtilis*. Their paramagnetic properties cause nanoparticles to be easily separated from liquids, recycled and reused, and possibly widely applied as a disinfectant in the water [13]. However, due to the chemically unstable property of Fe_3O_4, the nanoparticles are easily broken down in aquatic media, particularly in acidic conditions. Coating Fe_3O_4 with polymers such as silica and chitosan is an alternative technique to prevent the dissolution of the Fe_3O_4 in the media. Substitution of synthetic magnetite with natural magnetic particles is expected to produce more stable magnetic material and is prospective for the future due to low cost.

This study reports the application of impregnated AgNP on natural magnetic particles/chitosan (NMP/Chi) composites as antibacterial agents. The antibacterial activity tests of *E. coli* and *S. aureus* were performed with a well-diffusion method and in aqueous media. The magnetic particles provide easy separation of the agent from the aqueous media.

■ EXPERIMENTAL SECTION

Materials

The materials used were natural magnetic particles (NMP) isolated from iron sand collected from Glagah Kulon Progo beach, Yogyakarta, using a procedure reported by Nuryono et al. [14]. The chemicals used included hydrochloric acid (HCl 37%), sodium citrate ($Na_3C_6H_5O_7$, p.a), acetic acid (CH_3COOH 96%), silver nitrate ($AgNO_3$ 99.98%), and ammonia (NH_3 25%) purchased from Merck, technical chitosan from CV. Chi Multiguna. Other materials such as distilled water were obtained from CV. Progo. The antibacterial test using bacterial cultures, *E. coli*, *S. Aureus*, nutrient agar, and nutrient broth (NB) were conducted at the Faculty of Biology, Universitas Gadjah Mada.

Instrumentation

The non-analytical instruments used included laboratory glassware (Pyrex, Iwaki), a hotplate completed with a magnetic stirrer, mortar, oven (Memmert UN 55 53L), 200 mesh sieve. Analytical instruments used were an analytical balance (Mettler

622

Indones. J. Chem., 2022, 22 (3), 620 - 629

Toledo; Shimadzu AUW120), and universal pH (Merck). Characterization of all composite samples was performed with Fourier Transform Infrared spectrophotometer (FTIR; Shimadzu Prestige-21) and X-ray diffractometer (XRD; PANalytical X'Pert Pro series 2318 using Cu source). The AgNP in suspension was measured their absorbance with UV-Visible spectrophotometer (Shimadzu UV-1700) and Transmission Electron Microscope (TEM; JEOL series JEM-1400). The Scanning Electron Microscope-Energy Dispersive X-ray (SEM-EDX; Hitachi SU 3500) was used to identify the morphology and elemental composition of NMP/Chi/AgNP1.0.

Procedure

Synthesis of silver nanoparticles

AgNP samples were synthesized by reducing Ag(I) using sodium citrate, referring to the procedure reported by Fosso-Kankeu et al. [15]. A total of 50 mL of (0.5; 1.0; and 1.5 mM) $AgNO_3$ in an Erlenmeyer flask was heated at 100 °C for 1 h, then 5 mL of 1% sodium citrate was added dropwise. The mixture was stirred with a magnetic stirrer during heating until it turned pale yellow, indicating AgNP in suspension had been formed. AgNP samples were characterized with a UV-Visible spectrophotometer. The analysis with a UV-Visible spectrophotometer was carried out by measuring the absorbance at a 300–800 nm wavelength. The suspensions of AgNP obtained from 0.5, 1.0, and 1.5 mM $AgNO_3$ were called AgNP0.5, AgNP1.0, and AgNP1.5, respectively.

Preparation of HCl-activated NMP

Ten grams of iron sand was washed repeatedly and dried under sunlight for 48 h. Then, iron sand was separated using an external magnet. The separated iron sand was mashed and sieved with 200-mesh size. Iron sand (lower than 200 mesh) was rewashed using distilled water and dried in an oven for 18 h at 95 °C. Subsequently, 0.5 g of the sample was added with 1 mL of HCl 1 M, soaked for 15 min, and dried in an oven for 24 h at 95 °C.

Synthesis of composite NMP/Chi/AgNP

Typically, 0.15 g of chitosan was dissolved in a beaker glass in 30 mL of 1% acetic acid solution. Chitosan solution (30 mL) was added with 0.5 g of HCl-activated NMP then stirred for 5 h at room temperature (25 °C). The mixture was added with 0.5 M NH_4OH until pH of 7 (neutral) has achieved. Then the mixture was poured with 52 mL of AgNP suspensions which were prepared from all concentrations of $AgNO_3$ solution. The mixture was dried in an oven at a temperature of 60 °C for 24 h.

All NMP/Chi/AgNP prepared were characterized with FTIR and XRD. SEM-EDX and TEM were used to characterize NMP/Chi/AgNP1.0. For TEM analyses, the sample was prepared by dipping the copper grid into colloidal AgNP, then dried at room temperature. AgNP images were obtained at an accelerated voltage of 120 kV. FTIR characterization was performed to determine the functional groups of composites, and XRD was used to identify the electro-oxidation product of the sample phase according to the standard peak patterns of the ICDD card. SEM-EDX data was collected to identify the morphology and elemental composition.

Antibacterial activity test with well-diffusion method

After the equipment and material sterilizations, 1 mL of *E. coli* bacteria was taken using a micropipette and put in a liquid medium. Then, the bacteria were incubated for 24 h at 37 °C. The base media was poured into a petri dish, cooled, and stored until hardened for 1 h. Subsequently, the bacteria were evenly spread on the base media using a cotton swab. For the antibacterial test of NMP, NMP/Chi, and all prepared NMP/Chi/AgNP samples, one well was made in the agar medium with a diameter of ± 6 mm, which was put in the tested samples. After adding the tested samples, the petri dish was then incubated at 37 °C for 24 h. Antibacterial activity was calculated by their inhibition zone (in mm diameter). Similar work was also performed for *S. aureus.*

Antibacterial activity test in water

Antibacterial activity test in water was performed for NMP/Chi/AgNP1.0 composite with a shake flask turbidimetry method. The absorbance (turbidity/optical density) in aqueous media was measured with a UV-Vis spectrophotometer. Absorbance (turbidity/optical density) shows the number of bacteria contained in the media. Liquid media (150 mL) containing nutrient broth (1.3 g/100 mL) was mixed with 150 mg of

NMP/Chi/AgNP1.0 composite and was stirred for 1 min. At each particular interval time, the absorbance of the mixture was measured with a UV-vis spectrophotometer.

■ RESULTS AND DISCUSSION

Silver Nanoparticles (AgNP)

The concentration of silver nitrate ($AgNO_3$) as a precursor affects the number of AgNP formed. The investigation was conducted over the varied $AgNO_3$ concentrations (0.5, 1.0, and 1.5 mM). At the same condition, with a higher concentration of precursors, the reduction of silver nanoparticles occurs faster. In addition, the color change to darker at higher $AgNO_3$ concentration. $AgNO_3$ solution with the highest concentration (1.5 mM) produced the most concentrated color of AgNP suspension.

As shown in Fig. 1, the resulted AgNP could be identified by the wavelength profile of surface plasmon resonance (SPR). The maximum wavelength of SPR ranges from 400 up to 450 nm [16]. The absorbance at a wavelength of 416, 424, and 425 nm can be observed at the samples of 0.5, 1.0, and 1.5 mM, respectively. It means that the AgNP in suspension has been formed.

Based on Fig. 1, the increase in $AgNO_3$ concentration enhances the sample's absorbance gradually. The highest
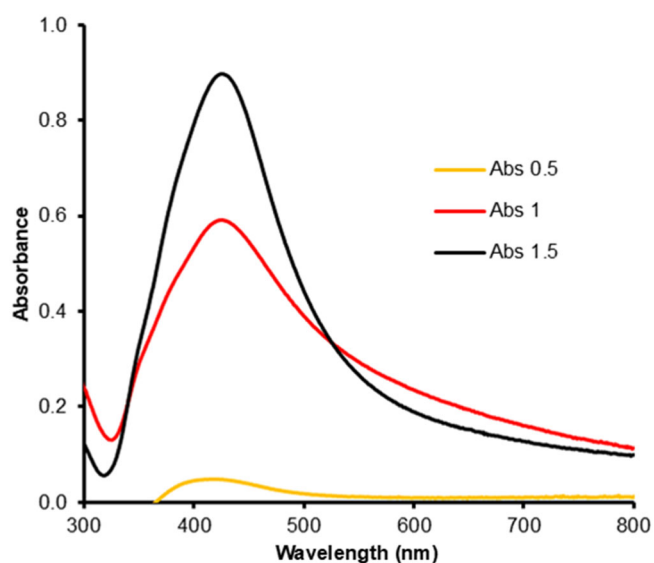
Fig 1. Absorbance at UV-Vis region of AgNP suspensions prepared from various concentrations of $AgNO_3$ solutions

absorbance was observed in the sample of 1.5 mM. However, the sample of 0.5 mM showed the lowest absorbance profile, which appeared at the wavelengths of 300 to 500 nm. It might be caused by a low concentration of $AgNO_3$ addition, thus producing a small AgNP quantity. Mulfinger et al. [17] stated that the low and high profile of the sample's absorbance reveals the amount of AgNP produced and the increase of the reaction rate. Herein, the resulted AgNP (sample 0.5 mM) could not be easily detected by using the spectrophotometer instrument.

Characteristics of NMP/Chi/AgNP

Functional groups

Composites of NMP/Chi/AgNP, including NMP and NMP/Chi, were characterized with FTIR to identify their functional groups in the samples and displayed in Fig. 2.

The O–H stretching vibrations of chitosan are observed at around 3000–3500 cm^{-1}, and C–H stretching appears at 2924 cm^{-1}, whereas O–H bending is at 1620 cm^{-1}. The N–H angular deformation on the CO–NH plane is observed at a wavenumber of 1543 cm^{-1}, and the C–O stretching at 1080 cm^{-1}. These results were similar to the previous data reported [18]. The sharp characteristic absorption peaks at wavenumbers 574 and 455 cm^{-1} correspond to the Fe–O bond of Fe_3O_4 in the NMP/Chi composite impregnated with AgNP (Fig. 2(c-e)), revealing that the composite is formed via in situ pathway [16].

Samples with the addition of various concentrations show the changes in their intensity, peak width, and wavenumber of some specific peaks of chitosan (Fig. 2(c-e)). The peak of –OH stretching moves to the small wavenumbers. Bonds between O–Ag and N–Ag are probably weakening the O–H and N–H hydrogen bonds. In contrast, at a wavenumber of 1080 cm^{-1}, the intensity of C–O stretching of C–OH chitosan increases. The large quantity of the acetyl group of chitin substituted by hydrogen atom into amine (–NH_2) leads to lower vibration energy and thus causes significant changes; a shift to the lower wavenumber of the amine group (–NH_2) is observed.
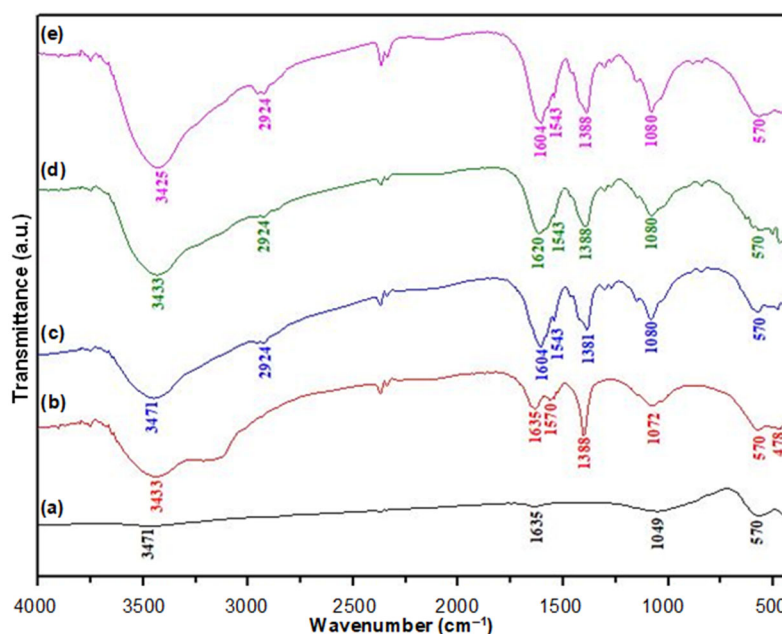
Fig 2. FTIR spectra of (a) NMP, (b) NMP/Chi, (c) NMP/Chi/AgNP0.5, (d) NMP/Chi/AgNP1.0, and (e) NMP/Chi/AgNP1.5, respectively

The absorption around 2924 cm^{-1} corresponds to the doubled C–H stretching, yet the presence of AgNP reduced single C–H stretching. It may be caused by the interaction between Ag nanoparticles with the groups of –OH and –NH$_2$ and then creating a stiffer chitosan structure, and the absorption intensity at 2924 cm^{-1} become much lower.

Structure of NMP/Chi/AgNP

The second characterization of the NMP/Chi/AgNP composite was carried out with X-ray diffraction. It is generally performed to identify the crystallinity and the present minerals. Additionally, it is performed to identify the phase of an electro-oxidation product by comparing it to the XRD pattern of NMP. The results obtained are presented in Fig. 3. As can be seen in Fig. 3, there are seven typical peaks of magnetite in NMP as the main content, which corresponds to an angle of 25° to 65° between the experimental XRD pattern of Fe$_3$O$_4$ in NMP and the standard XRD pattern of Fe$_3$O$_4$ (ICDD card no. 01-073-2273), namely at the angles 30°, 35°, 43°, 56°, and 62°. It indicates that Fe$_3$O$_4$ dominates the NMP component. The XRD pattern of NMP/Chi shows that the decreased peaks are observed at 30°, 35°, and 56°. In addition, new peaks at 27°, 29°, 31° appear and a peak at 35° decreases.

According to the Miller ICDD card no. 00-039-1894, those peaks belong to chitosan. The intensity of the prominent peak of chitosan is proportional to the quantity or amount and degree of crystallinity. Chitosan crystallinity is strongly influenced by the strength of chitosan polymer's intramolecular and intermolecular hydrogen bonds [19-20]. The chitosan crystallinity increases after being modified into NMP, probably due to the increased number of intramolecular and intermolecular hydrogen bonds.

The XRD patterns of NMP/Chi/AgNP with different AgNO$_3$ concentrations affect the composite crystallinity. It can be seen that the characteristic peak and intensity are broader and lower, respectively, with the increase in AgNP concentration. The broader peak indicates the heterogeneity of the polymer chains [21]. In addition, the increase in the AgNP concentration also causes an increase in the primary peak intensity of chitosan. Chitosan is a polymer with low crystallinity due to the loss of existing intramolecular and intermolecular hydrogen bonds. The AgNP at low concentrations can be involved in intramolecular and intermolecular hydrogen bonds, causing an increase in the crystallinity of NMP/Chi/AgNP composites. The
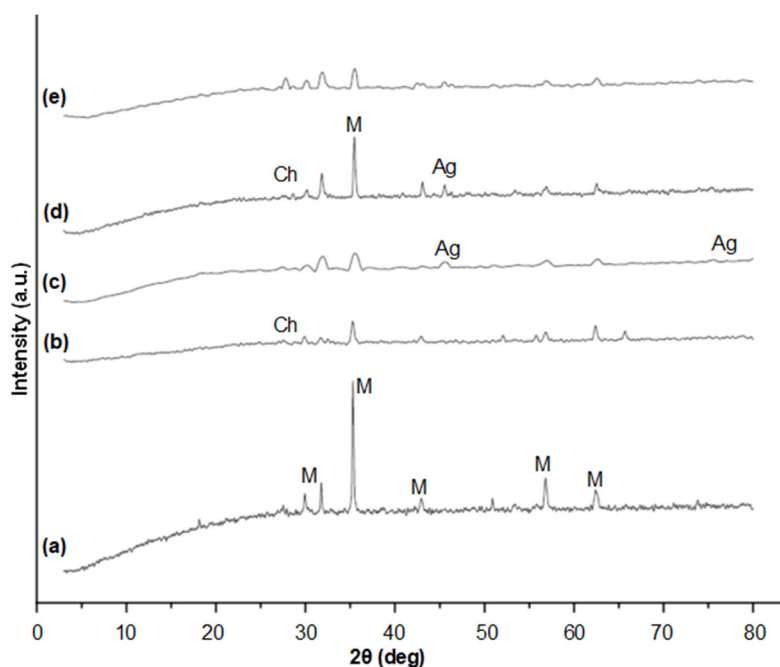
Fig 3. XRD patterns of (a) NMP, (b) NMP/Chi, (c) NMP/Chi/AgNP0.5, (d) NMP/Chi/AgNP1.0, (e) NMP/Chi/AgNP1.5, respectively

linking model of hydrogen bonding of chitosan and AgNP can be illustrated in Fig. 4.

Intermolecular interactions lead to regularity between polymer units, while intramolecular interactions lead to plane order of chitosan polymer units [18]. The AgNP impregnation causes to increase in the regularity of the chitosan crystal plane. The amount of AgNP used to replace intramolecular hydrogen bonds is more significant than that of intermolecular hydrogen bonds. The XRD pattern of NMP/Chi/AgNP shows that a peak intensity of 2θ about 31° is lower than NMP/Chi (before AgNP impregnation). The peak at 2θ 31° may be influenced more by intramolecular hydrogen bond interactions. Meanwhile, the peak intensity increase of 2θ around 27°, 30°, and 35° is probably due to the intermolecular interaction of hydrogen bonds of chitosan and NMP. The appearance of new peaks around 44° and 64° indicates AgNP peaks. As mentioned in the Miller ICDD card No. 01-089-3722, Ag metal has the *hkl* value of (111), (200), (220), (311) and (222) with 2θ of 38°, 44°, 64°, and 77°, respectively. It is reported that with the increasing number of metal ions bound by chitosan in the composite, the crystallinity index of chitosan decreased [22]. It is caused by the breakdown of intramolecular and
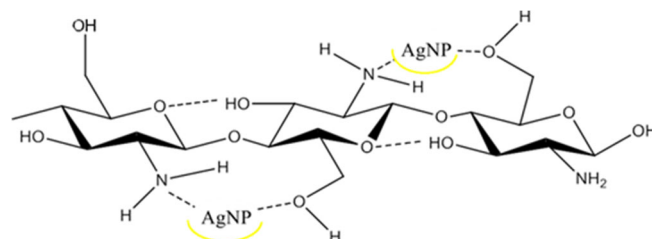

Fig 4. Substitution Model of intramolecular hydrogen bonds with AgNP

intermolecular hydrogen bonds, chitosan tends to form complexes, and Ag metal is not involved in intramolecular and intermolecular bonds.

Morphology of NMP/Chi/AgNP1.0

The morphology of NMP/Chi/AgNP1.0 characterized by Transmission Electron Microscope (TEM) is presented by AgNP1.0 and NMP/Chi/AgNP1.0, and the images can be seen in Fig. 5. From the image, the size distribution of each particle has been measured with ImageJ, and the average size is calculated. The result shows that the average size of AgNP in suspension and in the composite is 17.9 and 32.44 nm, respectively. The particle size of NMP is 47.02 nm, and the chitosan layering the NMP reaches 81.06 nm.
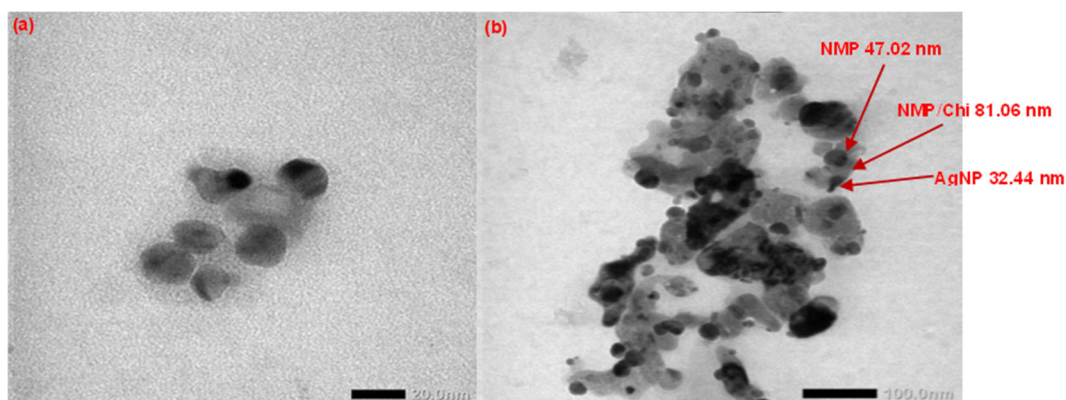
Fig 5. TEM images of (a) AgNP1.0 and (b) NMP/Chi/AgNP1.0

Scanning Electron Microscope (SEM) is used to observe the morphology of the NMP/Chi/AgNP composites. The SEM images of samples are presented in Fig. 6. The morphology of NMP/Chi/AgNP1.0 shows an uneven surface; there are rough bumps on the surface, whereas NMP/Chi (before AgNP impregnation) appears to have a smooth surface even when viewed up to 5000 times magnification. Additionally, there are no spots on the NMP/Chi surface, while NMP/Chi/AgNP shows white spots. The spots indicate AgNP in the sample.

The elemental composition in the samples investigated was analyzed with SEM-EDX, and the result is summarized in Table 1. This analysis may provide semi-quantitative data on elements in samples [23]. It can be seen that NMP/Chi/AgNP1.0 contains silver with an atomic percentage of 0.1%. The SEM-EDX data also show the presence of carbon, nitrogen, oxygen, and iron. The carbon and nitrogen contents come from chitosan, while the iron appears from iron oxide magnetite (Fe_3O_4) or hematite (α-Fe_2O_3). The percentage of C and N elements is higher in NMP/Chi/AgNP than in NMP.

Antibacterial Activity

The antibacterial activity of NMP/Chi/AgNP was carried out referring to the well-diffusion method. When the inhibition zone diameter of 5 mm or less, the activity can be categorized as weak, an inhibition zone of 5–10 mm as moderate, 10–20 mm is categorized as strong, and an inhibition zone of 20 mm or more is categorized as very strong [24]. The qualitative test results of the antibacterial activity of the samples can be seen in Fig. 7, and the activity based on the inhibition

Table 1. The results of EDX analysis on the composite of NMP/Chi/AgNP1.0

Element	NMP	NMP/Chi	NMP/Chi/AgNP1.0
C	4.54	15.99	22.14
N	0.41	6.42	8.43
O	51.73	30.30	32.42
Fe	15.44	3.99	3.28
Al	4.84	1.29	0.97
Si	14.65	5.36	4.52
Ag			0.10
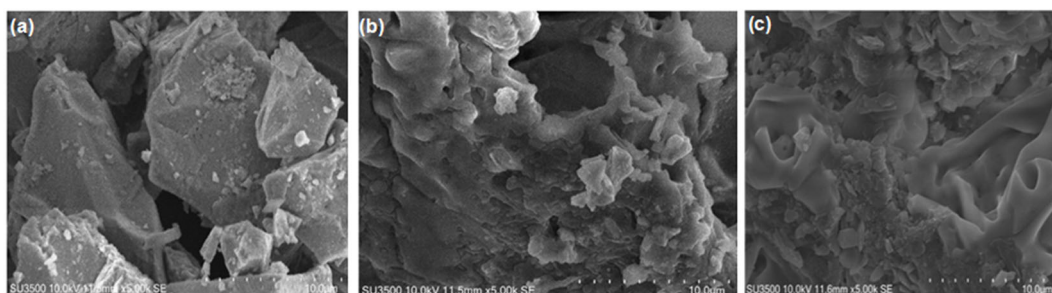
Fig 6. SEM images of composite (a) NMP, (b) NMP/Chi, and (c) NMP/Chi/AgNP1.0, with a magnification of 5000×
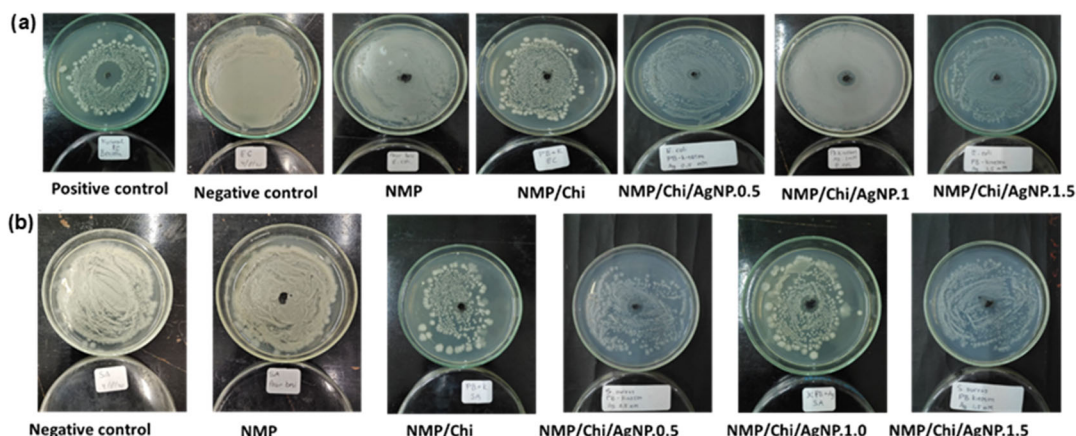
Fig 7. Images of antibacterial testing results for (a) *E. coli* and (b) *S. aureus* by measuring the diameter of the inhibition zone

Table 2. Measurements result of the inhibition zone diameter of bacteria

Antibacterial sample	Inhibition zone diameter (mm)		Category
	E. Coli	*S. Aureus*	
Negative control	0	0	Weak
NMP	0	0	Weak
NMP/Chi	7.56	9.62	Moderate
NMP/Chi/AgNP0.5	11.49	14.00	Strong
NMP/Chi/AgNP1.0	14.39	16.18	Strong
NMP/Chi/AgNP1.5	12.66	16.79	Strong
Positive control (betadine)	24.51	28.41	Very strong

zone measurement is summarized in Table 2. In Fig. 7, the colloidal AgNP indicates inhibitory activity against *E. coli* and *S. aureus* bacteria. The results showed that NMP/Chi/AgNP gives an antibacterial activity stronger than other tested samples. The highest inhibition zone diameter occurs in NMP/Chi/AgNP1.0, from AgNO$_3$ 1.0 mM, (14.39 mm) for *E. coli* and NMP/Chi/AgNP1.5, from AgNO$_3$ 1.5 mM for *S. aureus* (16.79 mm). NMP/Chi/AgNP composites tested are less active than the positive control (betadine), giving the zone diameter of 24.51 mm and 29.41 mm for *E. Coli* and *S. aureus*, respectively. The antibacterial activity of NMP/Chi/AgNP1.0 and NMP/Chi/AgNP1.5 is not significantly different for *S. aureus*; hence, the characterization is conducted only for NMP/Chi/AgNP1.0.

The lower activity of the AgNP impregnated is probably caused by the low distribution of the particles in the media. AgNP bound to chitosan resulted in the breakdown of intermolecular and intramolecular hydrogen bonds so that chitosan tends to form chelates with AgNP. The intermolecular and intramolecular hydrogen bonds that are no longer formed can reduce the interaction of the entry of the composite surface, namely the AgNP active site, with the bacterial cell surface, thereby reducing antibacterial activity. From Table 2, it can be seen that chitosan alone gives inhibitory activity even though it is lower than AgNP. The factor responsible for the lowest activity of NMP/Chi/AgNP1.5 is unclear. However, the higher concentration leads to the aggregation of the particles and reduces the activity. It agrees with previous research that silver with nanoparticle size has a higher bacterial inhibitory power [25]. Silver nanoparticles are chemically more reactive and more easily ionized than silver particles in large materials. Therefore, nanoparticles are indicated to have high antibacterial abilities. Silver ions interact with cells to prevent protein synthesis, decrease surface permeability, and ultimately cause cell death.

628

Indones. J. Chem., 2022, 22 (3), 620 - 629

Table 3. The bacterial growth in water without and with antibacterial agent NMP/Chi/AgNP1.0

Time (h)	Number of *E. coli* produced (CFU/mL)		Number of *S. aureus* produced (CFU/mL)	
	Without composite	With composite	Without composite	With composite
0	2.4	2.1	0.8	0.8
1	2.4	2.0	0.8	0.7
2	2.3	2.3	1.9	1.9
3	2.3	2.3	1.9	2.1
4	3.8	2.1	3.2	2.1
5	5.3	2.1	6.3	1.8
50	4.9	2.4	21.3	4.5

Antibacterial Activity of NMP/Chi/AgNP1.0 in Water

The antibacterial activity of NMP/Chi/AgNP in aqueous media was tested by comparing the growth of bacteria in water with and without the addition of composites. The bacteria's presence resulted in the media's turbidity, which could be measured by the turbidimetric method and presented in CFU/mL. The results of the calculation of the number of bacteria expressed in CFU/mL are shown in Table 3.

From Table 3, it appears that the bacteria grew after incubation lasted for 3 h. The effect of the composite as antibacterial inhibition was only visible starting at 4 h. For *E. coli* bacteria, growth is prolonged, and the addition of composites practically prevents bacteria from growing. Up to 50 h, the inhibition rate reaches 51%. In contrast to *E. coli*, *S. aureus* can grow well up to 50 h. The addition of NMP/Chi/AgNP in the media inhibited growth significantly, namely 80%.

■ **CONCLUSION**

It can be concluded that the NMP/Chi composite powder has been successfully made with black color and an irregular shape on the surface. AgNP1.0 impregnation on the NMP/Chi increased the average particle diameter from 17.88 to 32.44 nm. Antibacterial test with the well-diffusion method showed that NMP/Chi/AgNP1.0 effectively inhibits the growth of bacteria for both *E. coli* and *S. aureus*. In water media, the composite indicated similar antibacterial properties, and *S. aureus* growth revealed more significance to be inhibited than *E. Coli*. Therefore, a separable and effective antibacterial composite, NMP/Chi/AgNP is prospective to be applied in aquatic environments.

■ **ACKNOWLEDGMENTS**

■ **REFERENCES**

[1] Mohamadshafiee, M.R., and Taghavi, L., 2012, Health effects of trihalomethanes as chlorinated disinfection by products: A review article, *Int. J. Environ. Ecol. Eng.*, 6 (8), 545–551.

[2] Ghasemi, N., Jamali-Sheini, F., and Zekavati, R., 2017, CuO and Ag/CuO nanoparticles: biosynthesis and antibacterial properties, *Mater. Lett.*, 196, 78–82.

[3] Susanty, D., Santosa, S.J., and Kunarti, E.S., 2020, Antibacterial activity of silver nanoparticles capped by *p*-aminobenzoic acid on *Escherichia coli* and *Staphylococcus aureus*, *Indones. J. Chem.*, 20 (1), 182–189.

[4] Ke, C.L., Deng, F.S., Chuang, C.Y., and Lin, C.H., 2021, Antimicrobial actions and applications of chitosan, *Polymers*, 13 (6), 904.

[5] Kumar, U., Mishra, M., and Prakash, V., 2012, Assessment of antioxidant enzymes and free radical scavenging activity of selected medicinal plants, *Free Radicals Antioxid.*, 2 (3), 58–63.

[6] Setiyani, R., and Maharani, D.K., 2015, Pemanfaatan komposit kitosan ZnO-SiO$_2$ sebagai agen antibakteri terhadap bakteri *Staphylococcus aureus* pada kain katun, *Unesa J. Chem.*, 4 (2), 88–93.

[7] Ayad, M., Salahuddin, N., Fayed, A., Bastakoti, B.P., Suzuki, N., and Yamauchi, Y., 2014, Chemical design of a smart chitosan-polypyrrolemagnetite

nanocomposite toward efficient water treatment, *Phys. Chem. Chem. Phys.*, 16 (39), 21812–21819.

[8] Sukamto, Kamiya, Y., Rusdiarso, B., and Nuryono, 2021, "Highly effective magnetic silica-chitosan hybrid for sulfate ion adsorption" in *Sustainable Development of Water and Environment*, Eds. Jeon, H.Y., Springer International Publishing, New York, 203–216.

[9] Fahmiati, F., Nuryono, N., and Suyanta, S., 2017, Characteristics of iron sand magnetic material from Bugel Beach, Kulon Progo, Yogyakarta, *IOP Conf. Ser.: Mater. Sci. Eng.*, 172, 012020.

[10] Victor, S., Andhika, B., and Syauqiah, I., 2016, Pemanfaatan kitosan dari limbah cangkang bekicot (*Achatina fulica*) sebagai adsorben logam berat seng (Zn), *Konversi*, 5 (1), 22–26.

[11] Wang, L., Hu, C., and Shao, L., 2017, The antimicrobial activity of nanoparticles: Present situation and prospects for the future, *Int. J. Nanomed.*, 12, 1227–1249.

[12] Xu, F., Ma, L., Huo, Q., Gan, M., and Tang, J., 2015, Microwave absorbing properties and structural design of microwave absorbers based on polyaniline and polyaniline/magnetite nanocomposite, *J. Magn. Magn. Mater.*, 374, 311–316.

[13] Pachla, A., Lendzion-Bieluń, Z., Moszyński, D., Markowska-Szczupak, A., Narkiewicz, U., Wróbel, R.J., Guskos, N., and Żołnierkiewicz, G., 2016, Synthesis and antibacterial properties of Fe_3O_4-Ag nanostructures, *Pol. J. Chem. Technol.*, 18 (4), 110–116.

[14] Nuryono, N., Miswanda, D., Sakti, S.C.W., Rusdiarso, B., Krisbiantoro, P.A., Utami, N., Otomo, R., and Kamiya, Y., 2020, Chitosan-functionalized natural magnetic particle@silica modified with (3-chloropropyl)trimethoxysilane as a highly stable magnetic adsorbent for gold(III) ion, *Mater. Chem. Phys.*, 255, 123507.

[15] Fosso-Kankeu, E, De Klerk, C.M., van Aarde, C., Waanders, F., Phoku, J., and Pandey, S., 2016, Antibacterial activity of a synthesized chitosan-silver composite with different molecular weights chitosan against Gram-positive and Gram-negative bacteria, *International Conference on Advances in Science,* *Engineering, Technology & Natural Resources (ICASETNR-16)*, November 24-25, 2016, Parys, South Africa, 142–146.

[16] Cao, X., Shen, F., Zhang, M., and Sun, C., 2014, Rapid and highly-sensitive melamine sensing based on the efficient inner filter effect of Ag nanoparticles on the fluorescence of eco-friendly ZnSe quantum dots, *Sens. Actuators, B*, 202, 1175–1182.

[17] Mulfinger, L., Solomon, S.D., Bahadory, M., Jeyarajasingam, A.V., Rutkowsky, S.A., and Boritz, C., 2007, Synthesis and study of silver nanoparticles, *J. Chem. Educ.*, 84 (2), 322–325.

[18] Lin, Y.F., Chen, H.W., Chien, P.S., Chiou, C.S., and Liu, C.C., 2011, Application of bifunctional magnetic adsorbent to adsorb metal cations and anionic dyes in aqueous solution, *J. Hazard. Mater.*, 185 (2-3), 1124–1130.

[19] Caro, C., Castillo, P.M., Klippstein, R., Pozo, D., and Zaderenko, A.P., 2010, "Silver nanoparticles: Sensing and imaging application" in *Silver Nanoparticles*, Eds. Perez, D.P., IntechOpen, Rijeka, 201–223.

[20] Ioelovich, M., 2014, Cristallinity and hydrophility of chitin and chitosan, *J. Chem.*, 3 (3), 7–14.

[21] Sibilia, J.P., 1996, *A Guide to Materials Characterization and Chemical Analysis*, 2nd Ed., Wiley-VCH, New York.

[22] Modrzejewska, Z., and Kaminski, W., 1999, Separation of Cr(VI) on chitosan membranes, *Ind. Eng. Chem. Res.*, 38 (12), 4946–4950.

[23] Bindhu, M.R., and Umadevi, M., 2013, Synthesis of monodispersed silver nanoparticles using *Hibiscus cannabinus* leaf extract and its antimicrobial activity, *Spectrochim. Acta, Part A*, 101, 184–190.

[24] Davis, W.W., and Stout, T.R., 1971, Disc plate methods of microbiological antibiotic assay, *Appl. Microbiol.*, 22 (4), 659–665.

[25] Avicenna, S., Nurhasanah, I., and Kumaeni, A., 2021, Synthesis of colloidal silver nanoparticles in various liquid media using pulse laser ablation method and its antibacterial properties, *Indones. J. Chem.*, 21 (3), 761–768.